

Energy Partitioning in the Products of Ionic Decomposition

J. L. Franklin

For a unimolecular decomposition reaction to occur there must be sufficient energy in the decomposing molecule to surmount an energy barrier. Often this is no more than the bond dissociation energy, but sometimes there is an additional barrier. In either case, there may be excess energy ($E^* \geq 0$) to be distributed among the various modes of the reaction products. Understanding this energy distribution has been an important project for both theoreticians and experimentalists for many years. The problem is, of course, closely related to that of the rate of unimolecular reactions, and both have been subject to theoretical treatments having the same basis and set of assumptions. Unimolecular reaction rates have been well surveyed in recent publications (1, 2) and will not be treated here. Energy distribution in unimolecular reactions has been less extensively studied, and the greater part of the experimental work has been carried out by mass spectrometrists. The reason for this is that ions, because of their electric charge in the gas phase, are much more readily controlled and detected than are neutral species. Thus, the problem falls naturally into the domain of the mass spectrometrists.

Ionization in the gas phase can be brought about in several ways but is usually accomplished by either ultraviolet light or electrons and, at least with negative ions, the internal energy can be controlled over a fairly wide range. Ions also have the important advantage that their electric charge permits them to be deflected, retarded, or accelerated and, properly used, such operations can be made to yield the distribution of velocity.

It has been recognized for many years

that ions formed by fragmentation processes might have energies above their ground states and several studies have included measurements of translational energy. Thus, in an early study Blewett (3) determined both the appearance potential and kinetic energy of Br^- from Br_2 and deduced a very satisfactory value for the electron affinity of the bromine atom. Several other workers (4-11) measured the translational energies of fragment ions, mostly positive ions, and deduced the kinetic energy from the appearance potential to improve the thermochemical values deduced from their measurements. The best results were obtained with diatomic molecules, and no attempts appear to have been made until recently to relate translational energy to total excess energy.

We recognized that before energy partitioning could be understood it was necessary to obtain experimental data relating translational energy to total excess energy and that ionic decomposition reactions offered the best opportunity to accomplish this. Accordingly, we undertook the development of methods of measuring translational energy and the application of such methods to a variety of ionic processes.

Experimental Methods

Positive ions are formed under electron impact at higher electron energies and in greater abundance than are negative ions and so are generally easier to deal with. Consequently, we employed positive ions in the development of methods of measurement. We have employed two methods:

1) Analysis of the shapes of mass

peaks from a time-of-flight (TOF) mass spectrometer (12).

2) Variation in mass peak intensity with transverse electric field in a sector field mass spectrometer (13, 14).

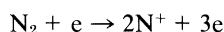
In a TOF instrument a pulse of electrons of short duration and controlled energy is passed through the ionization chamber. After it has passed a large extraction field is applied and the ions are swept from the source and accelerated to an energy of 3000 volts, with which they traverse the flight tube. They sort themselves into packets according to their ratio of charge to mass (e/m), the more massive taking longer than the less massive to reach the collector. The result is a time spectrum which can be interpreted in terms of mass since the flight time, t , is proportional to $m^{1/2}$. Now consider two ions formed in the electron beam with the same mass and energy, one with its initial trajectory directed toward and the other away from the collector. When the extraction pulse is applied the first will be accelerated toward the collector, while the second must be slowed to a halt and then reaccelerated toward the collector. When it reaches its original position it will lag behind the first by a few nanoseconds and will remain so all the way to the collector. The separation in time will, of course, depend on the initial energy of the two ions—the greater the energy the greater the separation. A packet having a large number of ions can be expected to exhibit a distribution of energies, which will be reflected in the shape of the mass peak.

In the sector field mass spectrometer ions are extracted from the ionization chamber continuously under the influence of a constant electric field. Since ions will be formed with an initial velocity the result is a curved trajectory in the source. Ions having small initial velocities will travel a relatively small transverse distance in leaving the source, whereas ions with large initial velocities will travel a relatively long distance and after leaving the source will be traveling at a relatively large angle to the axis of the analyzer. Two parallel electrodes are placed just after the ion gun and parallel

The author is Chairman of the Department of Chemistry and Welch Professor of Chemistry at Rice University, Houston, Texas 77001.

to the ion beam. A variable voltage is impressed across these electrodes. When the deflection voltage is varied ions of various initial energies are swept across the collector slit, and the resulting curve is related to the initial velocity distribution of the ions in question (15).

Both of the methods described above give precise reproducible results and agree rather well with each other. Both are capable of giving the average translational energy of an assemblage of ions in thermal equilibrium, although for the lighter ions a correction for gate width must be made with the TOF method. Some early measurements of translational energy by Hierl and Franklin (16) for N^+ from N_2 showed clearly the onset of the process



where e is an electron. The translational energy of N^+ at onset was large (4 eV), and when twice this was deducted from the electron energy at onset for the process fairly good agreement with spectroscopic data was obtained. Similarly, N^{2+} was formed with 5 eV of translational energy at its appearance potential of 63.63 eV. Again, when the translational energy was deducted the calculated value agreed within 0.3 eV with the spectroscopic value. Considering the very small intensity and large energies involved, this agreement was surprisingly good. Similar results were obtained with the ions from NO and CO (16).

At about this time a controversy arose over the correct value of the bond strength in fluorine, and we thought we could contribute by measuring the appearance potentials and translational energies at onset of the F^+ or F^- ions (or both) formed by dissociative resonance capture, dissociative ionization, and pair production processes. The results for the various processes agreed well with each other and supported the bond energy value $D^\circ(F_2) = 37.5 \pm 2.3$ kcal/mole (17).

Classical Statistics Applied to Energy Distribution

The fragments from diatomic molecules can have only electronic and translational energies. In most cases the fragments are formed in their ground electronic states, and when they are not the excited state can usually be readily deduced. Thus, in most instances all of the excess energy goes into translation. With molecules having more than two atoms this is not the case. If the molecule

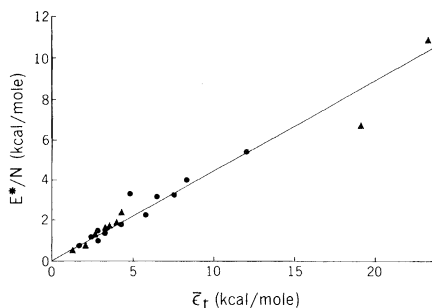


Fig. 1. Correlation of excess energy at onset, E^* , with the average translational energy in the center of mass, $\bar{\epsilon}_t$. (▲) Positive ions formed by dissociative ionization; (●) negative ions formed by dissociative resonance capture.

breaks into two fragments at least one of them will have vibrational and rotational degrees of freedom in addition to the translation that may be excited. Unfortunately, our techniques measure only translational energy directly, so it is necessary to find a way to relate our measured translational energies to total excess energy or to energy in the other internal modes.

A statistical treatment of the rates of unimolecular reactions was proposed by Rice and Ramsperger (18) and by Kassel (19), and, more recently, Eyring and his colleagues (20) have adapted it to isolated ionic systems. In this treatment the following assumptions are made:

- 1) The molecule is made up of a set of loosely coupled harmonic oscillators.
- 2) Vibrational energy is rapidly equilibrated among the various vibrational modes.
- 3) Rotation can be ignored.

With these assumptions we can write the distribution function for vibrational energy as

$$P(E^*, \nu) = \frac{\rho^\ddagger(E^*_{v,t} - \epsilon_t)}{\int_0^{E^*} \rho^\ddagger(E^*_{v,t} - \epsilon_t) d\epsilon_t} \quad (1)$$

where $P(E^*, \nu)$ is the vibrational distribution function for systems having excess energy E^* ; ρ^\ddagger is the density of vibrational states and, since rotation is ignored, is a function of $(E^*_{v,t} - \epsilon_t)$; $E^*_{v,t}$ is the excess of vibrational and translational energy of the reacting molecule over the energy of the fragments in their ground vibrational and translational states (however, one or more of the fragments may be electronically excited); and ϵ_t is the translational energy in the center of mass. The average value of ϵ_t is given by

$$\bar{\epsilon}_t = \frac{\int_0^{E^*} \epsilon_t \rho^\ddagger(E^*_{v,t} - \epsilon_t) d\epsilon_t}{\int_0^{E^*} \rho^\ddagger(E^*_{v,t} - \epsilon_t) d\epsilon_t} \quad (2)$$

In quasi-equilibrium theory the classical expression for the total number of vibrational states is

$$W(E^*) = \frac{(E^*_{v,t} - \epsilon_t)^{N-1}}{(N-1)! \prod_i h\nu_i} \quad (3)$$

and the density of vibrational states dW/dE^* , is

$$\rho^\ddagger = \frac{(E^*_{v,t} - \epsilon_t)^{N-2}}{(N-2)! \prod_i h\nu_i} \quad (4)$$

where $(N-1)$ is the number of vibrational modes in the transition state, h is Planck's constant, and the ν_i are vibrational frequencies. When Eqs. 3 and 4 are inserted into Eq. 2 and the integration is performed we find

$$\bar{\epsilon}_t = \frac{E^*_{v,t}}{N} \quad (5)$$

It may be assumed (13) that $\bar{\epsilon}_t$ arises from conversion of vibrational energy in the reaction coordinate to translational energy in crossing the barrier.

A theoretically much sounder evaluation of Eq. 2 would employ a summation of the vibrational states of the activated complex and, as will be discussed later, this has been done for several systems. However, for convenience we have employed the classical treatment above as a framework for correlating certain of our experimental results. We recognize that this is not a proper theoretical treatment, but it has proved exceptionally useful as a semiempirical method of treating some of our data and so we have felt justified in using it for this purpose.

In order to evaluate Eq. 5 it was necessary to obtain values of $E^*_{v,t}$ and $\bar{\epsilon}_t$. Values of $E^*_{v,t}$ could be obtained by carefully determining the appearance potentials for several fragmentation processes and deducting from them the appropriate heats of reaction; that is, $A_p - \Delta H_r = E^*$. Systems were chosen for which ΔH_r could be calculated from known thermochemical values. The translational energy was determined by one of the techniques described above at several values of the electron energy near onset and the curve was then extrapolated to onset. With positive ions it is necessary to determine $\bar{\epsilon}_t$ at onset, since at higher electron energies the leaving electrons take with them an undetermined amount of energy and so E^* is not known. The choice of fragmentation processes was subject to certain limitations; thus (i) the parent molecule could not have too many vibrational modes (< 30) if the translational energy were to be satisfactorily measured; (ii) the mass

of the fragment ion could not be excessive; and (iii) the neutral fragment could not be too light (it could not be hydrogen or deuterium) since the energy of the ion would be too small to measure.

With these limitations we chose several dissociative ionization processes for positive ions and several dissociative resonance capture processes for negative ions and measured their appearance potentials and translational energies at onset. It was, of course, necessary to correct for the thermal energy of the molecule being ionized, and this was done by means of the relationship

$$\bar{\epsilon}_i = \frac{m_i}{m_i + m_n} \left(\frac{3}{2} RT \right) + \frac{m_n}{m_i + m_n} \bar{\epsilon}_t \quad (6)$$

where the subscripts *i* and *n* refer to ion and neutral, respectively; $\bar{\epsilon}_i$ is the average energy in the center of mass; *R* is the gas constant; and *T* is absolute temperature.

The results (21, 22) are plotted in Fig. 1. The data are well fitted by a straight line, but the slope, which should be unity if Eq. 6 is correct, is 0.44. If we rewrite Eq. 6 with the empirically measured slope, α , included,

$$E^* = \alpha N \bar{\epsilon}_i \quad (7)$$

it will be apparent that α is a fraction and αN can be considered as the number of "active" vibrational modes. The fit of the line in Fig. 1 is quite good, but it is surprising that the fraction of active vibrations should be so nearly constant. Subsequent studies have shown that this is not always the case.

Thermochemical Values for Ions and Free Radicals

In view of the good fit of so many points to Eq. 7 with $\alpha = 0.44$, we thought it would be useful to take advantage of this correlation to measure the excess energy at onset and thus determine ΔH_f for several decomposition reactions. From this we could then compute the heat of formation of an ion or neutral fragment of interest. In this way we determined the heats of formation of several oxygen-containing free radicals and of several positive ions (23, 24); of several hydrocarbon- and nitrogen-containing free radicals and positive ions (25); and of the halogen molecular negative ions and several free radicals (26, 27). Time-of-flight mass spectrometers were employed and translational energies determined by peak shape analysis (21-24, 26, 27), and a sector field mass spectrometer was used and trans-

lational energy measured by the deflection method (25). In all cases an average value of 0.44 for α was employed. The results, given in Table 1, are in reasonable agreement with results obtained by other methods, where such values were available.

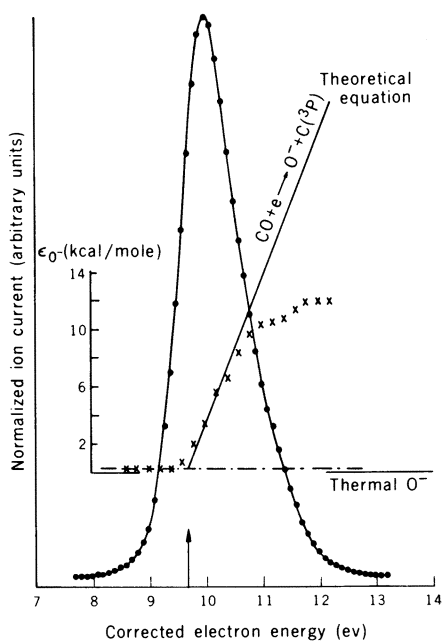
While the use of an average value of α at onset gave satisfactory empirical measurements of thermochemical properties, there was always the possibility that some systems would deviate seriously from the average. With improved instrumentation we accordingly set out to study the variation of $\bar{\epsilon}_i$ with E^* in each

of several molecular systems. This is possible with dissociative resonance capture produced by electrons or with pair production produced by photoionization, since in each case the energy introduced by the electron or the light remains with the system. We had only the electron capability, so our studies were limited to dissociative resonance capture processes. Since these are resonant processes they occur over only a limited energy range, usually 0.5 to 2.0 ev. Although this range is not very great, it provides room for quite large variations with most systems. Accordingly,

Table 1. Heats of formation of ions and radicals for reactions in which an average value ($\alpha = 0.44$) was used.

Compound	Ion	Radical	A_p (ev)	$\bar{\epsilon}_i$ (kcal/mole)	ΔH_f (kcal/mole)		Reference
					Ion	Radical	
HCOOH	HCO ⁺	OH	13.03	1.1	199		(23)
CH ₃ CHO	HCO ⁺	CH ₃	12.73	3.5	197		(23)
C ₂ H ₃ CHO	HCO ⁺	C ₂ H ₃	13.30	3.0	196		(23)
C ₂ H ₅ OH	CH ₃ OH ⁺	CH ₃	11.65	0.9	170		(23)
(CH ₃) ₂ O	CH ₃ O ⁺	CH ₃	11.95	4.6	164		(23)
CH ₃ ONO	CH ₃ O ⁺	NO	10.9	6.1	177		(23)
CH ₃ OC ₂ H ₅	C ₂ H ₅ O ⁺	CH ₃	11.30	2.4	141		(23)
CH ₃ OCH ₂ Cl	C ₂ H ₅ O ⁺	Cl	10.79	3.2	136		(23)
(CH ₃) ₂ CO	CH ₃ CO ⁺	CH ₃	11.32	2.5	148		(23)
CH ₃ COCl	CH ₃ CO ⁺	Cl	11.25	3.6	148		(23)
CH ₃ COOH	CH ₃ CO ⁺	OH	11.75	2.3	142		(23)
CH ₃ COOH	COOH ⁺	CH ₃	12.27	0	145		(23)
HCO ₂ CH ₃	CH ₃ O ⁺	HCO	12.23	2.7		7	(23)
HCO ₂ C ₂ H ₅	C ₂ H ₅ O ⁺	HCO	11.50	2.2		9	(23)
C ₂ H ₃ CHO	C ₂ H ₃ ⁺	HCO	13.64	2.1		8	(23)
HCO ₂ CH ₃	HCO ⁺	CH ₃ O	13.47	3.9		-2	(23)
CH ₃ CO ₂ CH ₃	CH ₃ CO ⁺	CH ₃ O	11.37	1.6		-3	(23)
CH ₃ ONO	NO ⁺	CH ₃ O	11.15	1.5		-4	(23)
C ₂ H ₅ ONO	NO ⁺	C ₂ H ₅ O	11.69	1.6		-6	(23)
CH ₃ OC ₂ H ₅	CH ₃ ⁺	CH ₃ OCH ₂	15.02	2.5		0	(23)
(CH ₃) ₂ CO	CH ₃ ⁺	CH ₃ CO	15.36	3.9		-2	(23)
CH ₃ COOH	CH ₃ ⁺	COOH	14.0	2.0		-58	(23)
HCO ₂ CH ₃	CH ₃ ⁺	HCO ₂	13.71	<2.2		≅ -46	(23)
CH ₃ NCS	CH ₃ ⁺	NCS	14.63	3.8		84	(21)
C ₂ H ₅ OH	H ₃ O ⁺	H + C ₂ H ₅ [*]	14.30	1.6(H ₃ O ⁺)	143		(24)
C ₂ H ₅ SH	H ₃ S ⁺	C ₂ H ₅	12.41	1.3	193		(24)
(CH ₃) ₂ S	H ₃ S ⁺	H + C ₂ H ₅ [*]	14.14	1.4(H ₃ S ⁺)	190		(24)
C ₂ H ₅ NH ₂	NH ₄ ⁺	H + C ₂ H ₅	12.72	1.9(NH ₄ ⁺)	148		(24)
CH ₂ Cl ₂	Cl ⁺	CH ₂ Cl	17.4	5.1		30.0	(26)
CH ₂ Br ₂	Br ⁺	CH ₂ Br	15.5	4.4		38.9	(26)
CH ₂ I ₂	I ⁺	CH ₂ I	13.2	3.0		52.4	(26)
CH ₃ C ₂ H	CH ₃ ⁺	HC ₂	15.57	3.6		130	(25)
1-C ₄ H ₈	CH ₃ ⁺	C ₃ H ₅	14.17	2.0		40	(25)
(CH ₃) ₂ CCH=CH ₂	CH ₃ ⁺	C ₅ H ₉	15.35	2.9		19	(25)
1-Butyne	CH ₃ ⁺	C ₃ H ₃	15.09	4.4		82	(25)
(CH ₃) ₃ CC≡CH	CH ₃ ⁺	C ₅ H ₇	14.74	2.5		59	(25)
(CH ₃) ₂ C=CH ₂	CH ₃ ⁺	C ₃ H ₅	16.39	4.6		53	(25)
1-C ₄ H ₈	C ₃ H ₅ ⁺	CH ₃	11.75	1.2	222		(25)
iC ₄ H ₈	C ₃ H ₅ ⁺	CH ₃	11.80	1.6	214		(25)
1-C ₄ H ₆	C ₃ H ₃ ⁺	CH ₃	11.71	1.3	263		(25)
CH ₃ NH ₂	CH ₃ ⁺	NH ₂	14.48	4.3		41	(25)
CH ₃ NH ₂	NH ₂ ⁺	CH ₃	15.92	3.8	304		(25)
(CH ₃) ₂ NH	CH ₃ ⁺	CH ₃ NH	14.79	3.1		43.6	(25)
(CH ₃) ₂ N	CH ₃ ⁺	(CH ₃) ₂ N	14.87	2.6		39	(25)
C ₂ H ₅ NH ₂	CH ₃ ⁺	CH ₂ NH ₂	15.61	4.4		43	(25)
(C ₂ H ₅) ₂ NH	CH ₃ ⁺	CH ₂ N(C ₂ H ₅)H	15.39	2.0		37	(25)
(C ₂ H ₅) ₂ N	CH ₃ ⁺	(C ₂ H ₅) ₂ NCH ₂	16.74	3.0		23	(25)
BF ₃	F ₂ ⁻	BF	10.2	23.2		-67	(27)
CCl ₄	Cl ₂ ⁻	CCl ₂	2.3	7.8		-58	(27)
CBr ₄	Br ₂ ⁻	CBr ₂	0.0	0.7		-59	(27)
CHI ₃	I ₂ ⁻	CHI	0.0	0.0		-55	(27)
CH ₃ CN	CN ⁻	CH ₃	2.1	2.2		25	(22)

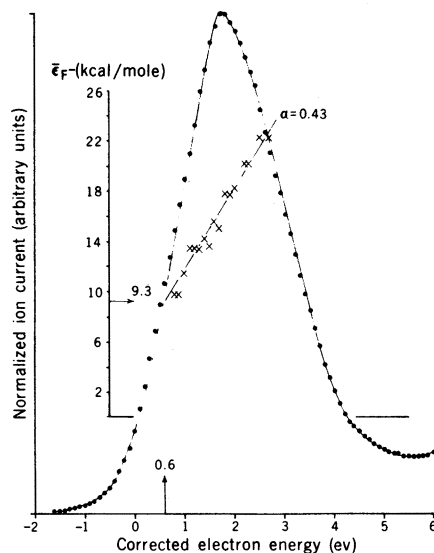
*Two-step process.



the same abscissa. The thermal energy limit for O^- is shown by the dot-dash line. The arrow represents the onset determined by deconvolution. Fig. 3 (right). (●) Resonance curve for F^- from NF_3 . (×) Translational energy ($\bar{\epsilon}_F$) of F^- from NF_3 . Both curves are plotted against the same abscissa. The arrows represent the onset determined by deconvolution.

we undertook to measure the translational energy of the ion across the resonance for several systems.

A typical ionization efficiency curve and plot of translational energy, ϵ_i , against electron energy are shown in Fig. 2. It should be noted that the resonance (ionization efficiency) curve is broadened because of the energy spread in the electron beam. This broadening has been eliminated by the computer deconvolution method of MacNeill and Thynne (28) based on an earlier method of Morrison (29). The onset determined by deconvolution is shown by an arrow in Fig. 2. The translational energy curve rises linearly with a slope of 12/28, as is required since the fragments are monatomic and all excess energy must go into translation. Similar behavior was observed with NO; thus, we were convinced that this method was satisfactory. We have also employed an iterative computer method for the deconvolution of the TOF mass peaks to obtain both translational energy distributions and average translational energies (30), and we recently applied a modification of the retarding potential difference (RPD) technique (31) in measuring both the resonance curves and the deflection curves for determining translational energy (32) on the sector field mass spectrometer. Both the deconvolution and RPD techniques gave improved results. In the RPD technique the electron beam is pulsed alternately at energies differing by a small amount (usually 0.05 to 0.1 eV) and the difference in intensities measured at various electron



energies until the appearance potential is reached. The method is useful in removing the curvature in the ionization efficiency curve near onset.

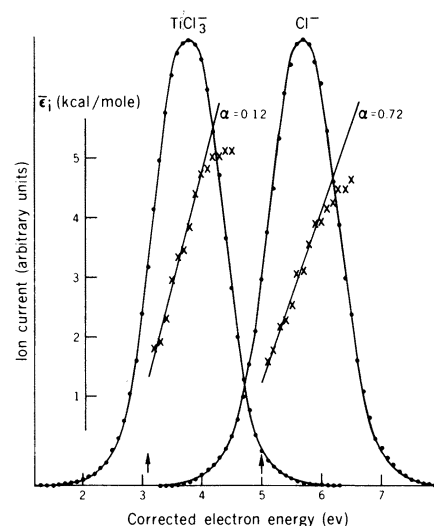
Figure 3 shows the resonance and translational energy curves for F^- from NF_3 (33). The resonance is unusually broad and the arrows show the onset obtained after deconvolution. Again the translational energy rises linearly across the resonance and from the slope we find $\alpha = 0.43$. The appearance potential occurs at the lower energy limit of the potential energy curve of the parent ion as determined by the Franck-Condon prin-

ple. This lower energy limit occurs well above the decomposition asymptote so that the decomposition occurs with considerable excess energy, 9.3 kcal/mole of which appears as translational energy of F^- . If the translational energy line is extrapolated to 0.9 kcal/mole (thermal energy), one obtains the electron energy that corresponds to the heat of reaction, in this case -19 kcal/mole, which enables us to calculate $\Delta H_f(NF_2) = 8.8$ kcal/mole, in excellent agreement with the accepted value. Only the neutral NF_2 can be vibrationally excited and in this case we find the vibrational energy at onset to be 20.1 kcal/mole. Within the energy resolution of our instrument we expect the vibrational energy also to increase linearly across the resonance. The behavior of this system is typical of many that we have studied by these techniques.

In Fig. 4 the resonance and translational energy curves for $TiCl_3^-$ and Cl^- from $TiCl_4$ are shown (34). The two ions are formed in quite different electron energy ranges. It is especially noteworthy that for the $TiCl_3^-$ ion $\alpha = 0.12$ and, since $TiCl_4$ has five atoms, $N = 9$, $\alpha N \approx 1$, and $\bar{\epsilon}_i \approx E^*$. Thus, essentially all of the excess energy has gone into translation. We have obtained almost identical results with the MX_3^- ion ($M = \text{metal}$ and $X = \text{halide}$) from several tetrahedral MX_4 compounds. It is clear from these results that vibrational energy is not equally distributed; in fact, with these processes it is not distributed at all. In these systems it is probable that the MX_3^- ion retains its tetrahedral structure and hence that no distribution of vibrational energy occurs.

On the other hand, α for the formation of Cl^- is unusually large (0.72), indicating that the vibrational energy, if not completely distributed, is nearly so, as might be expected if the MX_3 moiety changed its structure during decomposition, probably to a trigonal planar configuration. Similar results were obtained with the X^- ion from several MX_4 compounds. It seems evident that Cl^- and $TiCl_3^-$ arise from different electronic states of $TiCl_4$ and that this may be the cause of the difference in vibrational energy distribution in the two processes. However, as will be observed in Table 2, Cl^- and $SnCl_3^-$ exhibit very similar behavior, yet their appearance potentials differ by only 0.3 eV and so they probably arise from the same electronic state of $SnCl_4^-$.

The translational energy of Cl^- in Fig. 4 is very nearly thermal at onset and from the α we compute $E_{v,t}^*$ to be 8.2 kcal/mole at onset. Now the heats of formation of $TiCl_4$, $TiCl_3$, and Cl^- are known (35) and when these are com-



puted. This lower energy limit occurs well above the decomposition asymptote so that the decomposition occurs with considerable excess energy, 9.3 kcal/mole of which appears as translational energy of F^- . If the translational energy line is extrapolated to 0.9 kcal/mole (thermal energy), one obtains the electron energy that corresponds to the heat of reaction, in this case -19 kcal/mole, which enables us to calculate $\Delta H_f(NF_2) = 8.8$ kcal/mole, in excellent agreement with the accepted value. Only the neutral NF_2 can be vibrationally excited and in this case we find the vibrational energy at onset to be 20.1 kcal/mole. Within the energy resolution of our instrument we expect the vibrational energy also to increase linearly across the resonance. The behavior of this system is typical of many that we have studied by these techniques.

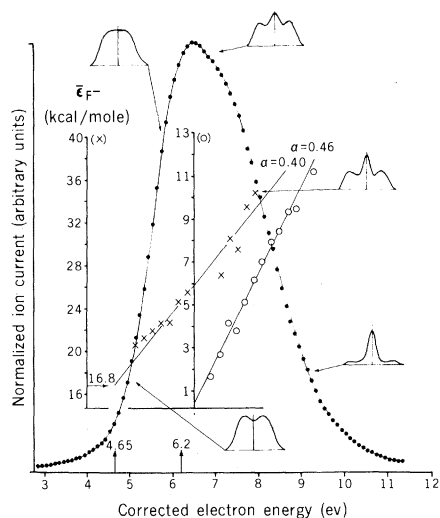
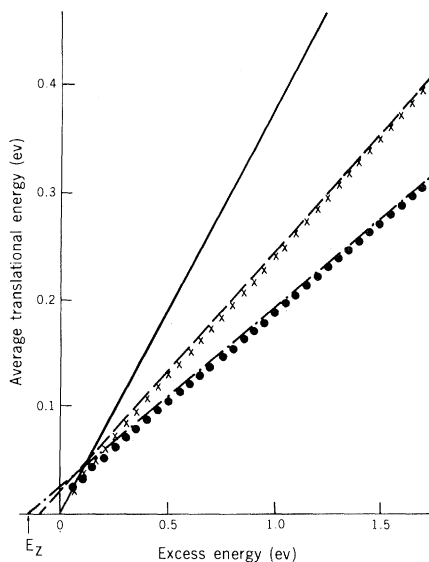


Fig. 5 (left). Curves of overlapping resonances of F^- from CF_4 and the approximate translational energies of F^- for the two processes. Note the changing shape of the mass peak with increasing electron energy; this shows the development of a second process giving F^- with a small translational energy and the decay of the process giving F^- with a large translational energy with increasing electron energy. The arrows on the abscissa indicate the onsets of the two processes. All curves are plotted against the same abscissa. Fig. 6 (right). Translational energy in the center of mass plotted against excess energy for P_2^- from P_4 . (Solid line) Experimental curve (58). (●) Values calculated by direct count of states from QET (48), Eq. 2. (×) Values calculated by direct count of states from phase space treatment (48), Eq. 10. (Dashed lines) Upper limits calculated from Eqs. 11 and 12.



proximate value for the second onset was deduced. Although the result was not as accurate as would be desired, it showed definitely that CF_3 was formed in the ground electronic state with large vibrational and translational energy at the lower electron energy, but in a quasi-thermal but electronically excited state at higher energy. The electronic transition for the excited CF_3 was approximately 4 to 4.3 eV.

We have studied the negative ions from a considerable number of compounds and the results are summarized in Table 2. Electron affinities and heats of formation of several species have been established. A surprising number of products appear to be formed in electronically excited states and in most of these the transition energy has been determined.

Several other investigators have studied the energy partitioning in dissociative resonance capture processes. Chantry has measured the translational energy distribution in O^- from CO_2 (37) and O^- from N_2O (38). Schulz and associates (39-41) have studied O^- from CO_2 . Chantry and Schulz (42) have measured the kinetic energy distribution in O^-O_2 along with the appearance potential in order to determine the electron affinity of O. The experimental devices used by these workers employed electron beams with a narrow energy spread (0.05 to 0.1 eV) and thus they were capable of detecting details that we have not been able to detect until recently. There has been gener-

al agreement between their work and ours, but there is one exception. Schulz and co-workers (40, 41) have shown the various vibrational levels with which CO is formed together with O^- from CO_2 . They did not measure the translational energy of O^- in these experiments. However, $E^* = \bar{\epsilon}_v + \bar{\epsilon}_t$, and at all points across the resonance their values of $\epsilon_v \approx E^*$, so translational energy would appear to be small in these experiments. The early work of Schulz (39) and that of Chantry (37) and our own results disagree with this. We do not understand this disagreement but suspect that Schulz's recent experiments may have discriminated seriously against ions of high kinetic energy.

Tests of Statistical Theories

So far we have taken advantage of an empirical relationship to obtain several thermochemical and electronic transition values. Comparison of the values obtained for α shows that the classical statistical treatment usually does not give results that agree with experiment. We have accordingly employed some of our data along with more sophisticated statistical treatments in an effort to ascertain whether agreement between theory and experiment might be found.

We early recognized that the assumption of the quasi-equilibrium theory that a decomposing molecule is a set of loosely coupled harmonic oscillators is not satisfactory. Also, as stated above, a sound

evaluation of Eq. 2 would employ a direct count of vibrational states to determine the density of states. We applied such a treatment including zero point energies to the fragmentation of several positive ions for which we had experimental data (43). The results, while somewhat closer to the experimental values than those obtained with Eq. 5, were not in satisfactory agreement for higher translational energies but were in fair agreement at values of $\bar{\epsilon}_t \approx 2$ to 3 kcal/mole. Several ions were treated as both loose and tight complexes. The latter gave somewhat better agreement with experiment but the agreement for the higher-energy systems was not satisfactory. I will show below that a direct count of states also fails to give agreement with experiment for kinetic energy release in dissociative resonance capture processes.

On the other hand, a number of investigators have successfully employed the direct count of states to predict the rates of decomposition of positive ions and from them to compute the relative intensities of mass spectral fragment ions (44). The computations of the various rate constants employed the same direct count of vibrational energy and states used by Spatz *et al.* (43) in computing the translational energies. We do not understand why this statistical treatment gives good results in the evaluation of rate constants and poor results in the evaluation of energy partitioning. However, the statistical theory is now generally accepted as the correct explanation of the rate of ionic decomposition.

Many mass spectra include so-called metastable peaks. In magnetic instruments these occur at nonintegral masses and are due to fragment ions formed in the analyzer. Thus they result from decomposition of long-lived metastable species. Cooks *et al.* (45) have shown that the widths and shapes of these peaks can be used to deduce the translational energy released during decomposition and with the use of the equation

$$k = \nu \left(1 - \frac{E^\ddagger}{E} \right)^{N-1} \quad (9)$$

have been able to deduce the activation energy of the reaction. Here ν is a frequency and E^\ddagger and E are activation energy and total energy, respectively. Where the heat of reaction is known, it is possible to ascertain whether the reverse reaction involves an energy of activation and, if it does, to determine its magnitude. The reverse reaction is, of course, an ion-molecule one, and the activation energies of several such reactions have been determined in this way.

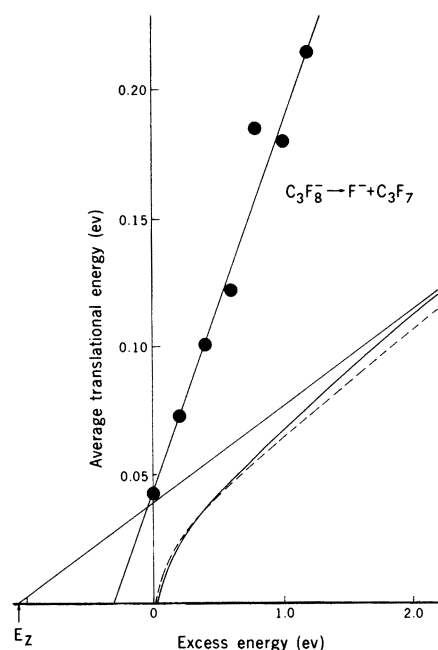


Fig. 7. Translational energy in the center of mass plotted against excess energy for F^- from C_3F_8 . (●) Experimental points (33). (Dashed line) Values calculated by direct count of states from QET (48), Eq. 2. (Curved solid line) Values calculated by direct count of states from phase space treatment (48), Eq. 10. (Straight solid line) Upper limit for classical QET treatment, Eq. 11.

In a further effort to improve the statistical treatment of energy release, Klots (46) has derived Eq. 10 for the average translational energy. Klots employed the quasi-equilibrium hypothesis for the reverse ion-molecule reaction to form a loose transition state and microscopic reversibility to derive the translational energy in the unimolecular fragmentation. He assumed that angular momentum is small. He argued that this is equivalent to the phase-space formalism (47)

$$\bar{\epsilon}_t = \frac{F_t \int_0^{E^*} \rho(\epsilon_v)(E^* - \epsilon_v)^{S+1} d\epsilon_v}{\int_0^{E^*} \rho(\epsilon_v)(E^* - \epsilon_v)^S d\epsilon_v} \quad (10)$$

where ρ is the density of vibrational states in the products and F and S are constants that depend only on the geometry of the reacting system. If the classical density of states is employed with Eq. 10, the expression reduces to $\bar{\epsilon}_t = E^*/N'$, where N' differs from N , the number of oscillators in the parent ion, by no more than 2. Thus, for O^- from CO_2^- , $N = 3$. In this formulation $N' = 2.5$, corresponding to an α of 0.83 in our terminology. Measurements in our laboratory yield an αN of approximately 1.5. Thus, in the classical approximation Eq. 10 does not predict the experimental results. With more complex molecules having a larger number of vibrational degrees of free-

dom, the $\bar{\epsilon}_t$'s calculated by the phase space and quasi-equilibrium methods will approach each other and both will in most cases give values considerably less than the experimental ones.

It was mentioned above that translational energies of positive ion fragmentation processes were computed by using a complete count of vibrational states. The data employed were necessarily limited to the energies at onset, and thus the variation of translational energy over a range of excess energy in a single system could not be determined. As shown above, this is readily accomplished with negative ions formed by dissociative resonance capture processes. Accordingly, Carter (48) has calculated the translational energies for several such processes by both Eqs. 2 and 10, using a direct count of states and including the zero point energies as discussed by Whitten and Rabinovitch (49). The results with the direct count of states agrees with those obtained with the classical distribution function, except at small vibrational energies (less than about twice the average zero point energy). The upper limits of the translational energy according to the quasi-equilibrium theory (QET) (Eq. 2) and the phase space theory (Eq. 10) may be written as

$$\bar{\epsilon}_t < = \frac{E^* + E_z}{N} \quad (\text{QET}) \quad (11)$$

$$\bar{\epsilon}_t < = \frac{E^* + E_z'}{N'} \quad (\text{phase space}) \quad (12)$$

where E_z is the zero point energy of the activated complex and E_z' is the sum of the zero point energies of the products.

Figures 6 and 7 compare experimental results for the processes P_2^- from P_4 and F^- from C_3F_8 with values calculated from Eqs. 2 and 10 by employing direct counts of states. The upper limits of $\bar{\epsilon}_t$ calculated from Eqs. 11 and 12 are also shown. Although the values calculated with the phase space theory (Eq. 10) are somewhat larger than those calculated with the quasi-equilibrium theory (Eq. 2), neither gives results in agreement with experiment.

Trajectory Calculations

In view of the consistent failure of statistical models to predict translational energies, Carter (48) has approached the problem by the use of classical trajectory calculations. The calculations were applied to the O^-CO_2 process and were based on a model that approached as nearly as possible to CO_2^- (50). By computing the results of a large number of

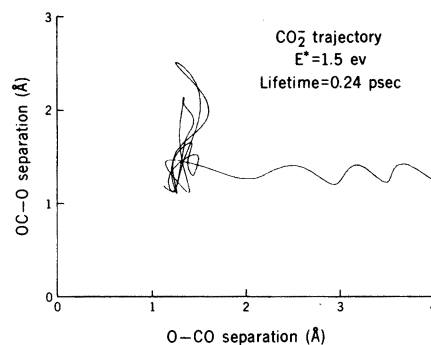


Fig. 8. Typical trajectory for the separation of O^- from CO_2^- .

trajectories, it became possible to compare the dynamic results to those of statistical theories applied to the model. Bunker (51), Kuntz *et al.* (52), and others have made similar trajectory calculations but with little emphasis on energy partitioning in unimolecular processes.

Earlier, Le Roy (53) pointed out that the translational energies of positive ions obtained by Haney and Franklin (21) and by DeCorpo *et al.* (22), which were not in agreement with statistical theories, could be understood in terms of a dynamic or rate process. Our later data on negative ions are much better suited to the evaluation of the dynamical treatment because of the availability of a range of energies from the same system.

In these computations Carter (48) assumed that CO_2^- was formed with the ground state configuration of CO_2 , but with various amounts of excess energy. Several trajectories were obtained with each value of E^* and the average distributions of translational, vibrational, and rotational energy were calculated. A typical trajectory is given in Fig. 8. In Fig. 9 the results of 200 such trajectories are plotted as points for comparison with curves of translational energy by the quasi-equilibrium and phase space methods. The QET results fall below the trajectory calculations and the phase space results fall below but closer to the trajectory results. Lines showing the results obtained by Hadley (30) using data of Harland (54) by the TOF method and data of Carter (32) by the deflection method are also shown. Although the results by the two experimental methods differ slightly, both, especially below $E^* = 1$ ev, are in rather good agreement with the trajectory calculations. Above $E^* = 1$ ev the trajectory results scatter badly and tend to fall below the experimental curves. We do not understand this behavior at the higher excess energies. If we compare the fraction of excess energy in rotation, vibration, and translation as determined by the phase space and trajectory methods, we find that for $E^* = 1$ ev

both methods give about 40 percent in vibrational energy, but the trajectory method gives 55 percent in translation and only 5 percent in rotation, whereas the phase space calculation gives 40 percent in translation and 20 percent in rotation.

It is obvious that much remains to be done both experimentally and theoretically if energy partitioning is to be understood. It is desirable to make dissociative resonance capture measurements with an electron beam of narrow energy spread. Schulz and co-workers (40, 41) have made a beginning by measuring the resonance curve of O^- from CO_2 with an electron beam having a full width at half-maximum of 0.05 eV; they were able to detect three vibrational states of the product CO. However, they did not measure translational energies and their intensities were so small that it was necessary to average for a very long time. We have made a start at measuring both resonance curves and translational energies by using a modification of the RPD technique (31) as was mentioned above. The energy resolution, although less than that of Schulz, seems quite good and offers promise of giving much better results than have been possible previously.

Our translational energy data taken by the peak shape analysis and deflection methods agree quite well at low energies ($\epsilon_i < 13$ kcal/mole) but in some cases differ considerably at higher energies. This failure appears to be instrumental in origin and may well result from the two methods of collecting ions from the ionization chamber. The TOF instrument collects ions whose initial trajectories are parallel to the flight tube, whereas the sector field instrument collects ions whose initial trajectories are perpendicular to the analyzer. It is known that some processes do not occur isotropically but prefer certain orientations to the electron beam (55, 56). We have designed an instrument to measure ion intensities and energies as a function of angle of flight relative to the electron beam. Translational energies would be determined by the retarding potential method, which has the advantage of being independent of the orientation of the initial trajectory of the ion.

Carter's initial trajectory studies have given much better agreement with experimental results than have any of the statistical methods we have applied. Unfortunately, the computational problem increases exponentially with the number of atoms in the molecule and becomes almost unsurmountable for molecules having five or more atoms. Ultimately, the trajectory calculations should be based on quantized vibrations.

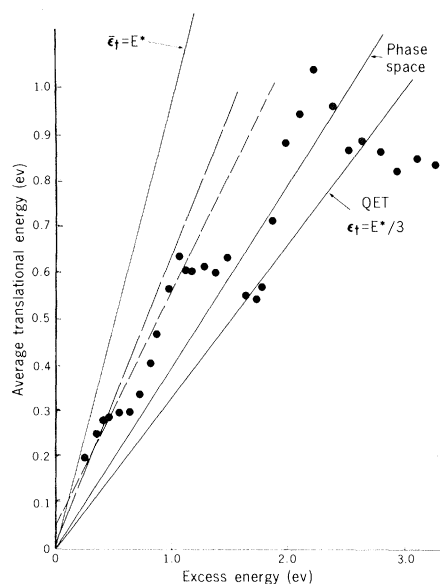


Fig. 9. Experimental and calculated curves for translational energy in the center of mass plotted against excess energy. (Solid lines) Values calculated by QET and phase-space theory and for the case $\epsilon_i = E^*$. (●) Values resulting from trajectory calculations (48). The line made up of long dashes represents experimental results obtained by the deflection method (32); that of short dashes represents experimental results obtained by peak shape analysis (30).

Thus, while much progress has been made, it is clear that both experimental and theoretical studies that probe deeper into the decomposition process are needed if energy partitioning is to be understood.

References and Notes

- For an extensive discussion see P. J. Robinson and K. A. Holbrook, *Unimolecular Reactions* (Wiley Interscience, New York, 1972).
- W. Forst, *Theory of Unimolecular Reactions* (Academic Press, New York, 1973).
- J. P. Blewett, *Phys. Rev.* **49**, 900 (1936).
- H. D. Hagstrum and J. T. Tate, *ibid.* **59**, 354 (1940).
- H. D. Hagstrum, *Rev. Mod. Phys.* **23**, 185 (1951).
- R. E. Fox and J. A. Hipple, *Rev. Sci. Instrum.* **19**, 462 (1948).
- J. A. Hipple, *Phys. Colloid Chem.* **52**, 456 (1948).
- R. J. Kandel, *J. Chem. Phys.* **22**, 1496 (1954); *Phys. Rev.* **91**, 436 (1953).
- C. A. McDowell and J. W. Warren, *Discuss. Faraday Soc.* **10**, 53 (1952).
- J. D. Waldron, *Trans. Faraday Soc.* **50**, 102 (1954).
- C. E. Berry, *Phys. Rev.* **78**, 597 (1950).
- J. L. Franklin, P. M. Hieryl, D. A. Whan, *J. Chem. Phys.* **47**, 3148 (1967).
- R. Taubert, *Z. Naturforsch. Teil A* **19**, 484 (1964).
- , *Adv. Mass Spectrom.* **1**, 489 (1959); J. Bracher, H. Ehrhardt, H. Fuchs, R. Osberghaus, R. Taubert, *ibid.* **2**, 285 (1963).
- D. K. Sen Sharma and J. L. Franklin, *Int. J. Mass Spectrom. Ion Phys.* **13**, 139 (1974).
- P. M. Hieryl and J. L. Franklin, *J. Chem. Phys.* **47**, 3154 (1967).
- J. J. DeCorpo, R. P. Steiger, J. L. Franklin, J. L. Margrave, *ibid.* **53**, 936 (1970).
- O. K. Rice and H. G. Ramsperger, *J. Am. Chem. Soc.* **49**, 1672 (1927); *ibid.* **50**, 617 (1928).
- L. S. Kassel, *J. Phys. Chem.* **32**, 225 and 1065 (1928); in *Kinetics of Homogeneous Gas Reactions* (Chemical Catalog Co., New York, 1932). See also (1) for a complete treatment of the Rice-Ramsperger-Kassel theory and subsequent extensions of it.

- H. M. Rosenstock, M. B. Wallenstein, A. L. Wahrhaftig, H. Eyring, *Proc. Natl. Acad. Sci. U.S.A.* **38**, 667 (1952).
- M. A. Haney and J. L. Franklin, *J. Chem. Phys.* **48**, 4093 (1968).
- J. J. DeCorpo, D. A. Bafus, J. L. Franklin, *ibid.* **54**, 1592 (1971).
- M. A. Haney and J. L. Franklin, *Trans. Faraday Soc.* **65**, 1794 (1969).
- , *J. Chem. Phys.* **50**, 2028 (1969).
- D. K. Sen Sharma and J. L. Franklin, *J. Am. Chem. Soc.* **95**, 6562 (1973).
- J. J. DeCorpo, D. A. Bafus, J. L. Franklin, *J. Chem. Thermodyn.* **3**, 125 (1971).
- J. J. DeCorpo and J. L. Franklin, *J. Chem. Phys.* **54**, 1885 (1971).
- K. A. G. MacNeill and J. C. J. Thynne, *Int. J. Mass Spectrom. Ion Phys.* **3**, 35 (1969).
- J. D. Morrison, *J. Chem. Phys.* **39**, 200 (1963).
- F. J. Hadley and J. L. Franklin, *Int. J. Mass Spectrom. Ion Phys.* **18**, 249 (1975).
- R. E. Fox, W. M. Hickam, D. J. Grove, T. Kjeldaa, *Rev. Sci. Instrum.* **26**, 1101 (1955); *Phys. Rev.* **84**, 859 (1951).
- D. E. Carter, unpublished results.
- P. W. Harland and J. L. Franklin, *J. Chem. Phys.* **61**, 1621 (1974).
- S. L. Bennett, R. E. Pabst, J. L. Margrave, J. L. Franklin, *Int. J. Mass Spectrom. Ion Phys.* **15**, 451 (1974).
- JANAF Thermochemical Tables, *Natl. Stand. Ref. Data Ser. Natl. Bur. Stand.* **37** (1971).
- P. W. Harland, J. L. Franklin, D. E. Carter, *J. Chem. Phys.* **58**, 1430 (1973).
- P. J. Chantry, *ibid.* **57**, 3180 (1972).
- , *ibid.* **51**, 3369 (1969).
- G. J. Schulz, *Phys. Rev.* **128**, 178 (1962).
- A. Stamatovic and G. J. Schulz, *Phys. Rev. A* **7**, 589 (1973).
- D. Spence and G. J. Schulz, *J. Chem. Phys.* **60**, 216 (1974).
- P. J. Chantry and G. J. Schulz, *Phys. Rev.* **156**, 134 (1967).
- E. L. Spatz, W. A. Seitz, J. L. Franklin, *J. Chem. Phys.* **51**, 5142 (1969).
- For an excellent summary of this topic, see M. L. Vestal, in *Fundamental Processes in Radiation Chemistry*, P. Ausloos, Ed. (Interscience, New York, 1968), pp. 59–118.
- R. G. Cooks, J. H. Beynon, R. M. Caprioli, G. R. Lester, *Metastable Ions* (Elsevier, New York, 1973).
- C. E. Klots, *Z. Naturforsch. Teil A* **27**, 553 (1972); *J. Phys. Chem.* **75**, 1526 (1971).
- P. Pechukas and J. C. Light, *J. Chem. Phys.* **42**, 3281 (1965); J. C. Light, *Discuss. Faraday Soc.* **44**, 15 (1967).
- D. E. Carter, in preparation.
- G. Z. Whitten and B. S. Rabinovitch, *J. Chem. Phys.* **38**, 2466 (1963).
- Since our knowledge of CO_2^- is limited, it was necessary to use approximate equilibrium bond angles and bond lengths and the energy dependence of bond angles as obtained by M. Kraus and D. Neuman [*J. Chem. Phys. Lett.* **14**, 26 (1972)] from ab initio calculations, the asymmetric stretch frequency from matrix isolation measurements of K. O. Hartman and I. C. Hisatsune [*J. Chem. Phys.* **44**, 1913 (1966)], and the well depth as obtained experimentally by T. O. Tierman and R. P. Clow [*Adv. Mass Spectrom.* **6**, 295 (1974)] and from calculations by Kraus and Neuman.
- D. L. Bunker, *J. Chem. Phys.* **37**, 393 (1962); *ibid.* **40**, 1946 (1964).
- P. L. Kuntz, E. M. Nemeth, J. L. Polanyi, *ibid.* **50**, 4607 (1969).
- R. L. Le Roy, *ibid.* **53**, 846 (1970); *ibid.* **55**, 1476 (1971).
- P. W. Harland, unpublished results.
- R. J. Van Brunt and L. Kieffer, *Phys. Rev. A* **2**, 1899 (1970).
- , *ibid.* **10**, 1633 (1974).
- S. L. Bennett, J. L. Margrave, J. L. Franklin, J. E. Hudson, *J. Chem. Phys.* **59**, 5814 (1973).
- S. L. Bennett, J. L. Margrave, J. L. Franklin, *ibid.* **61**, 1647 (1974).
- J. Ling-Fai Wang, J. L. Margrave, J. L. Franklin, *ibid.*, p. 1357.
- R. E. Pabst, D. Perry, J. L. Margrave, J. L. Franklin, *Proc. 23rd Annu. Conf. Mass Spectrom.* (1975), p. 153.
- J. Ling-Fai Wang, J. L. Margrave, J. L. Franklin, *J. Chem. Phys.* **60**, 2158 (1974).
- S. L. Bennett, J. L. Margrave, J. L. Franklin, *J. Inorg. Nucl. Chem.* **37**, 937 (1975).
- I wish to express my appreciation for support from the Robert A. Welch Foundation and the Office of Naval Research (contract N00 14-75-C-0415). I also wish to express my gratitude to my co-authors and to the *Journal of Chemical Physics* for permission to reproduce Fig. 3 and to the *International Journal of Mass Spectrometry and Ion Physics* for permission to reproduce Fig. 4.